

Supporting Information

High-rate free-standing $\text{Na}_3\text{V}_2(\text{PO}_4)_3$ symmetric full cell for sodium-ion batteries

*Milan K. Sadan, Minyeong Jeon, Jimin Yun, Eunji Song, Kwon-Koo Cho, Jou-Hyeon Ahn, and Hyo-Jun Ahn **

^aResearch Institute for Green Energy Convergence Technology, Gyeongsang National University, 501 Jinju-daero, Jinju, Gyeongnam 52828, Republic of Korea

^bDepartment of Materials Engineering and Convergence Technology, RIGET, Gyeongsang National University, 501 Jinju-daero, Jinju, Gyeongnam 52828, Republic of Korea

E-mail: ahj@gnu.ac.kr (H. Ahn)

Experimental Section

Synthesis of free-standing NVP electrode

Free-standing NVP electrodes were synthesized by a simple and scalable method. The precursor solution was prepared by dissolving sodium hydroxide (NaOH, 98%, Alfa Aesar, USA), ammonium dihydrogen phosphate ($\text{NH}_4\text{H}_2\text{PO}_4$, 99%, Acros Organics, Belgium), ammonium vanadium oxide (NH_4VO_3 , 99%, Alfa Aesar), and citric acid ($\text{C}_6\text{H}_8\text{O}_7$, 98%, Sigma Aldrich, United States) in deionized (DI) water. After complete dissolution, the solution was heated at 120 °C for 6 h to evaporate the solvent, and finally, a precursor was obtained. The obtained precursor was then powdered using a mortar and pestle. 2.46 g of polyacrylonitrile (PAN, Sigma Aldrich, MW= 150,000) and 1 g of the precursor were dispersed in 20 ml of dimethylformamide (Sigma Aldrich). The solution was then subject to electrospinning at room temperature at a flow rate of 1 mL h⁻¹ and a voltage of 12 kV. The obtained electrospun mat was then stabilized in an air atmosphere at 250 °C for 3 h, followed by carbonization at 800 °C for 3 h in a N₂ atmosphere. The obtained mat was directly used as an electrode without further treatment. For comparison, carbon nanofiber is synthesized the same method without an NVP precursor.

Material characterization

The structural characterization of the free-standing NVP was characterized by X-ray diffractometry (XRD) using a Bruker D8 diffractometer (Bruker Corporation, USA). The morphology was observed using a combination of field-emission scanning electron microscopy (FESEM) and transmission electron microscopy (TEM). The tools used for FESEM and TEM were TESCAN MIRA3 (LM, Czechia) and JEOL 2010 FEG (JEOL Ltd., Japan), respectively. The carbon content was analyzed using thermogravimetric analysis (TGA, Q50 TA Instruments) in an air atmosphere.

Electrochemical characterization

The electrochemical performance was analyzed using a free-standing electrode without any binder and conducting agent with an active material (NVP) loading of 1 mg cm⁻². The high loading of 3.5 mg cm⁻² and 6.5 mg cm⁻² are also studied. Sodium foil was used as the counter and reference electrodes. Sodium hexafluorophosphate (1 M NaPF₆) in an ethylene glycol dimethyl ether (DME) and Sodium perchlorate (1M NaClO₄) in ethylene carbonate (EC): propylene carbonate (PC) mixture (1:1 V%) with 5% fluoroethylene carbonate (FEC) electrolyte were prepared in-house. Glass fiber filter paper (GF/D, Whatman PLC, UK) and Celgard 2400 were coupled together for use as separators. The cells were assembled in an argon-filled glove box and tested at room temperature. Cell cycling was performed using a galvanostat (WBCS 3000 L, WonA Tech Co. South Korea). In contrast, cyclic voltammetry and electrochemical impedance spectroscopy were performed using a VMP3 multichannel potentiostat (Biologic, Seyssinet-Pariset, France). The electrochemical performance of the NVP cathode was analyzed in the voltage window of 1.9-4.0 V and NVP anode in 1-2.3 V respectively. The galvanostatic intermittent titration technique (GITT) was carried out at a current rate of 50 mA g⁻¹ with a rest time of 12 minutes and 6 minutes subsequent charge/discharge. The symmetric full cell was assembled with a Na₃V₂(PO₄)₃ cathode to anode mass ratio of 1:2.4. The capacity of the full cell was calculated based on the mass of the cathode in the voltage window of 0.5-2.4 V. The anode and cathode half cells were cycled at 50 mA g⁻¹ for the first cycle before assembling the full cells to avoid irreversible capacity loss.

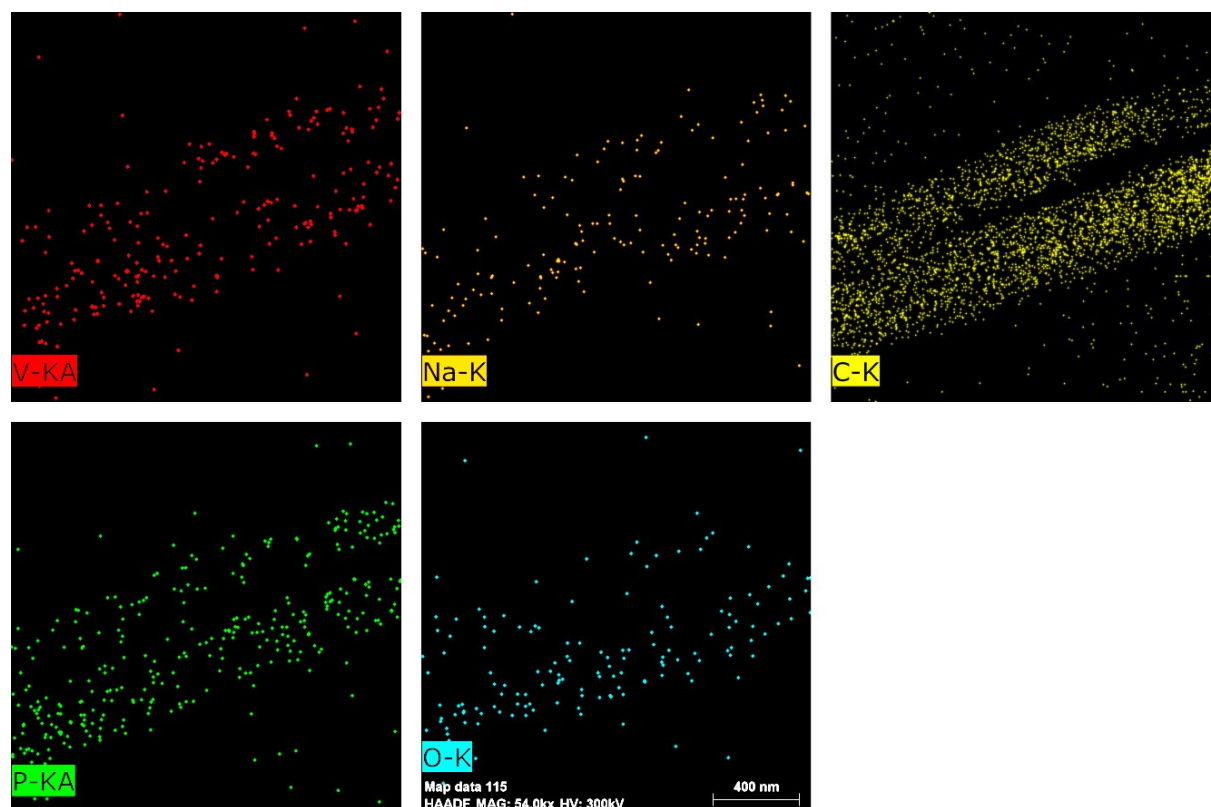


Figure S1. EDS mapping of NVPCNF electrode.

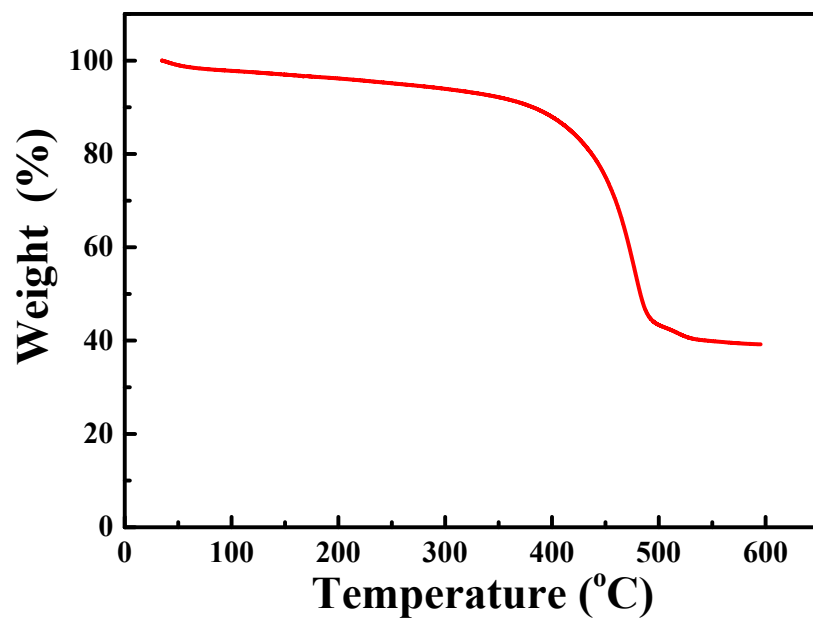


Figure S2. TGA of NVPCNF in air atmosphere.

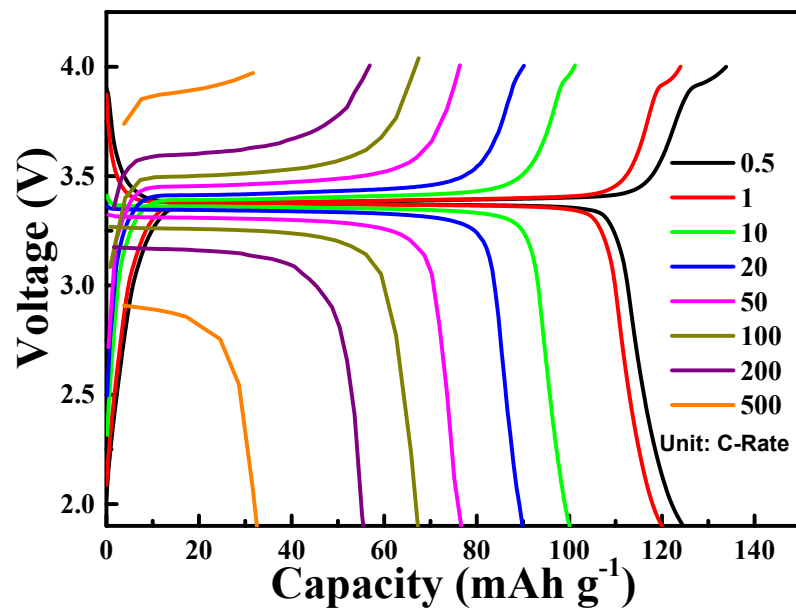


Figure S3. Voltage profile of NVPCNF cathode at the different current rates while rate performance.

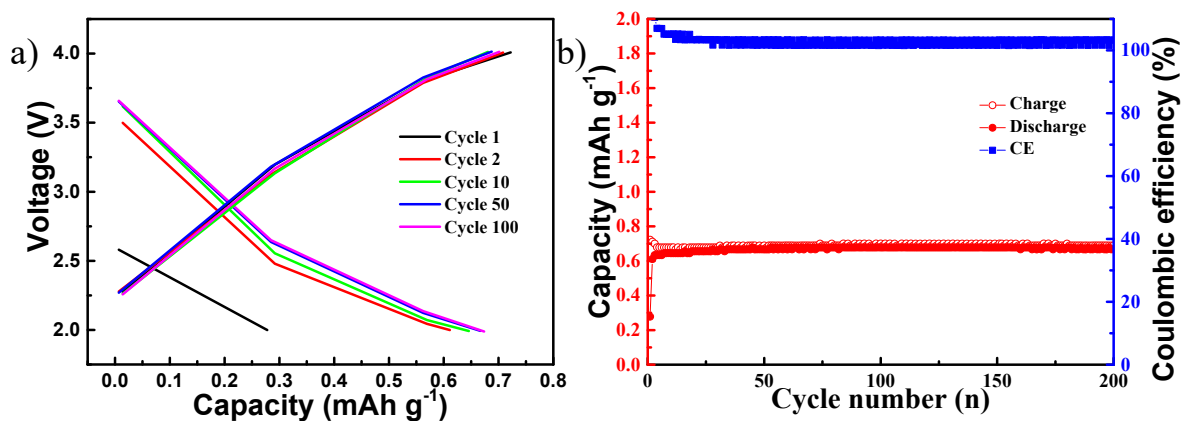


Figure S4. a) Voltage profile and cycling performance of carbon nanofiber at a current rate of 117 mA g^{-1} in the cathode voltage window.

The reversible capacity of the carbon nanofiber in the cathode voltage window is 0.6 mAh g^{-1} . By considering the 62 % of carbon in the NVPCNF electrode, the maximum capacity CNF can contribute is 0.96 mAh g^{-1} which is negligible capacity.

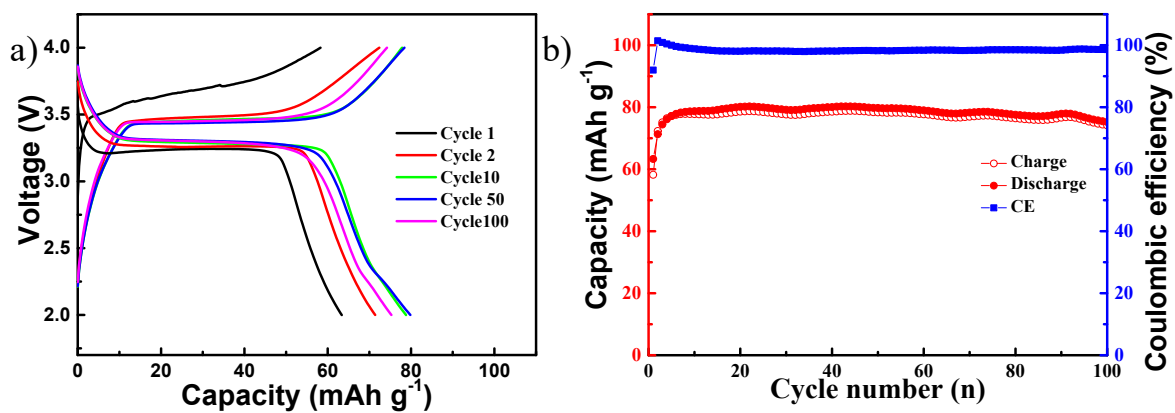


Figure S5. a) Voltage profile and b) cycling performance of the NVPCNF cathode in the carbonate-based electrolyte at 1C rate.

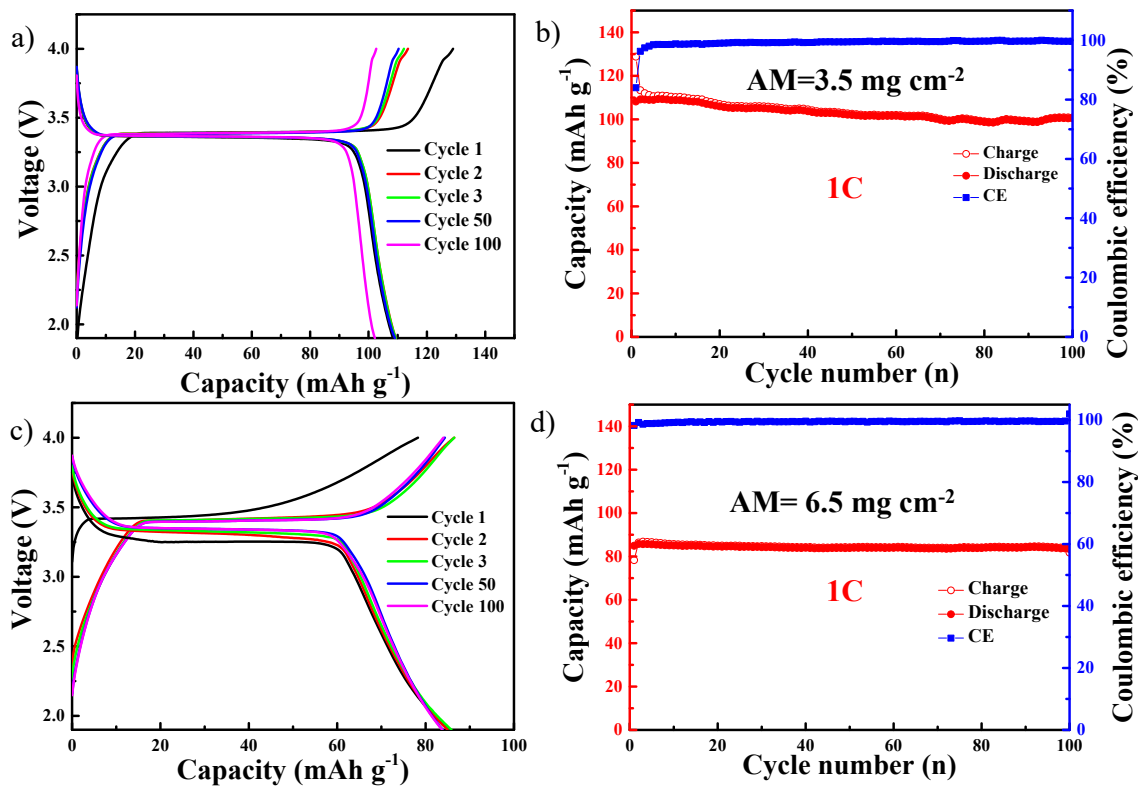


Figure S6. a, c) Voltage profile and b, d) cycling performance of the NVP cathode at high loading at 1 C rate.

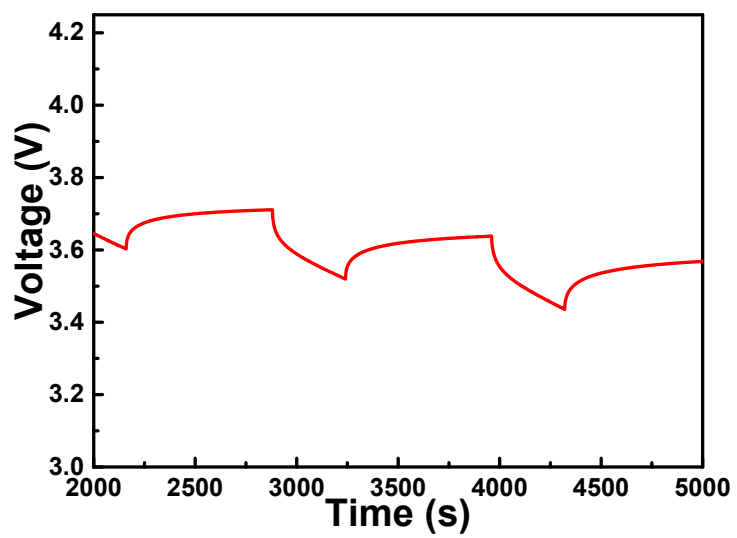


Figure S7. Galvanostatic Intermittent Titration Technique (GITT) curve of the NVPCNF cathode.

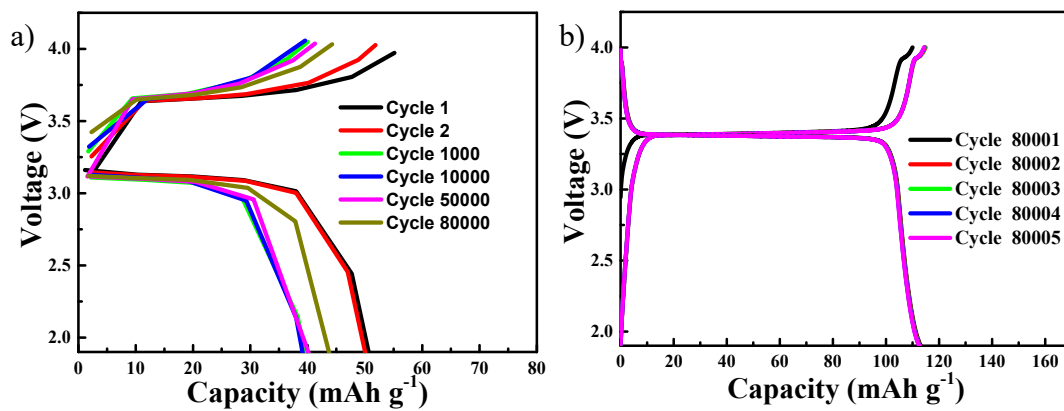


Figure S8. a) Voltage profile of NVP cathode while long-term cycling at a 200 C-rate, and b) voltage profile at 0.5 C rate after 80000 cycles.

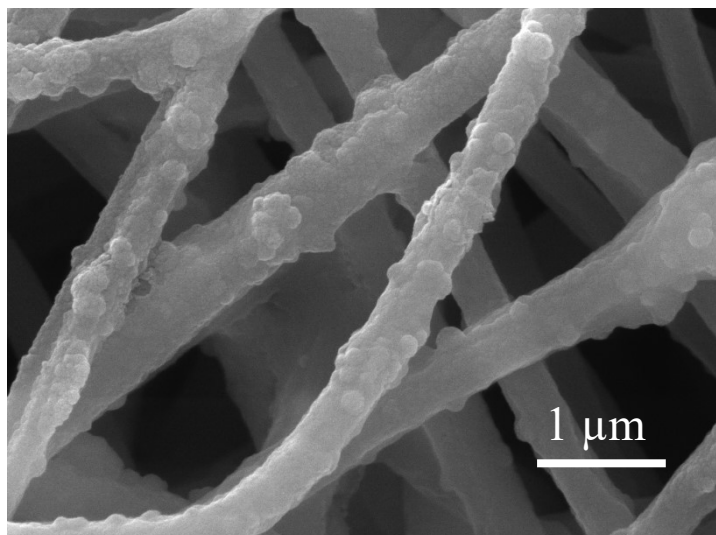


Figure S9. FESEM image of NVPCNF cathode after 80000 cycles.

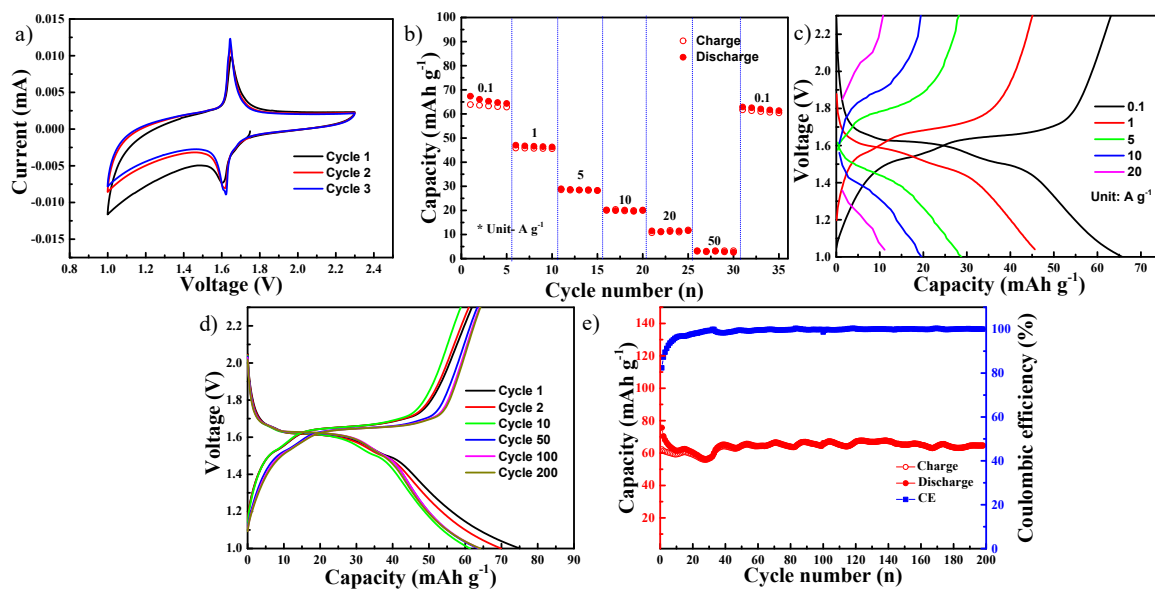


Figure S10. a) Cyclic voltammetry of the flexible NVP anode at a scan rate of 0.1 mV sec⁻¹, b) rate performance and c) corresponding voltage profile at different current rates, c) voltage profile and d) corresponding cycling performance of the flexible NVP at a current rate of 100 mA g⁻¹.

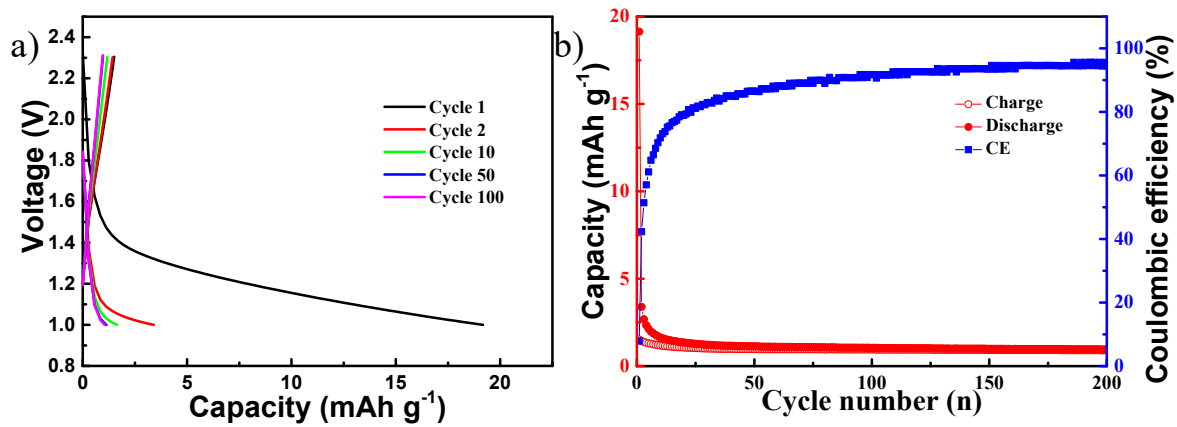


Figure S11. a) Voltage profile and b) cycling performance of the carbon nanofiber anode at a current rate of 100 mA g^{-1} .

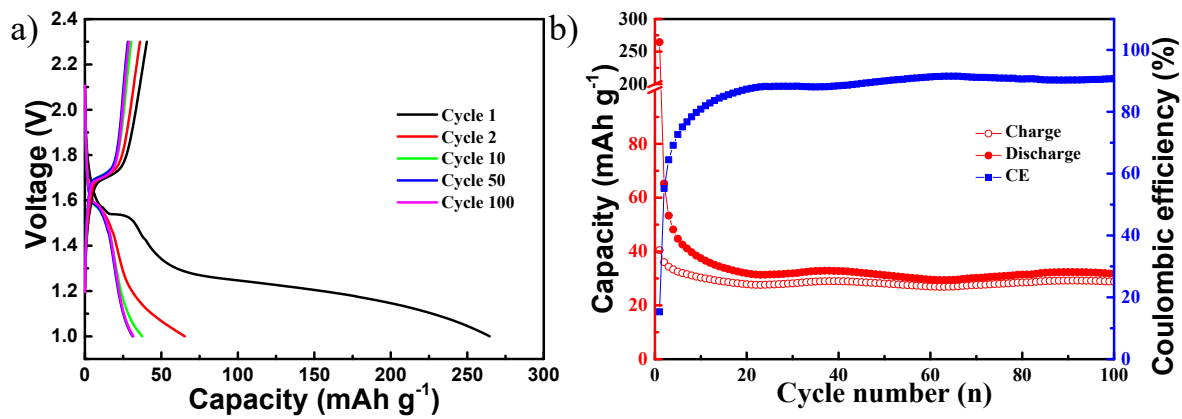


Figure S12. a) Voltage profile and b) cycling performance of the NVPCNF cathode in the carbonate-based electrolyte at a current rate of 100 mA g^{-1} .

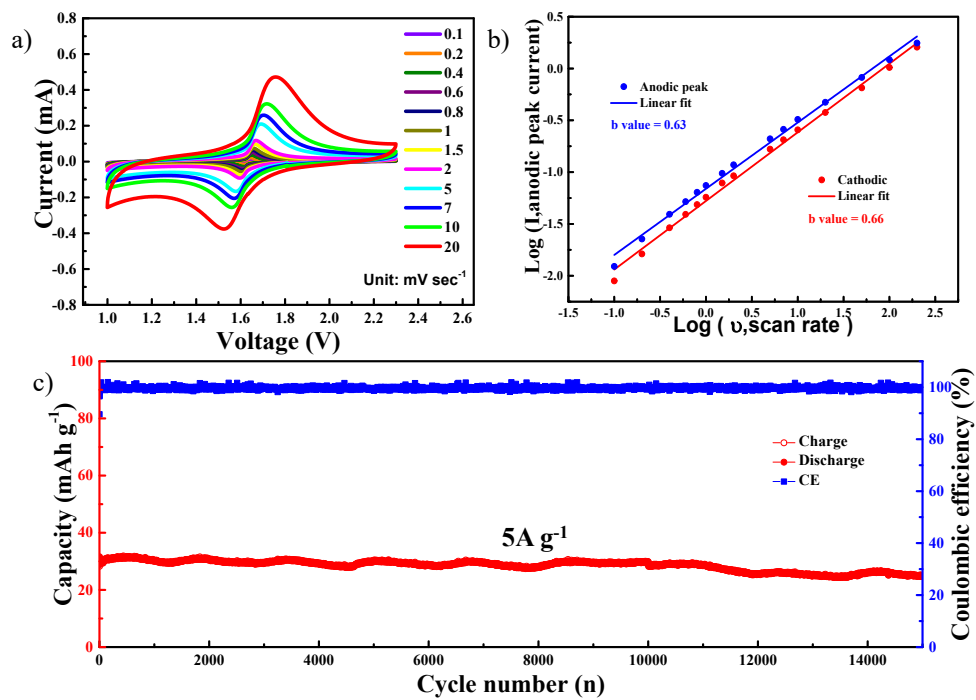


Figure S13. a) cyclic voltammetry of the flexible NVP anode at different scan rates from 0.1 to 100 mV sec⁻¹, b) Linear fitting of I_p versus $\nu^{1/2}$ curves from the redox peaks in CV curves, and c) long term cycling performance of the NVP anode at a current rate of 5 A g⁻¹.

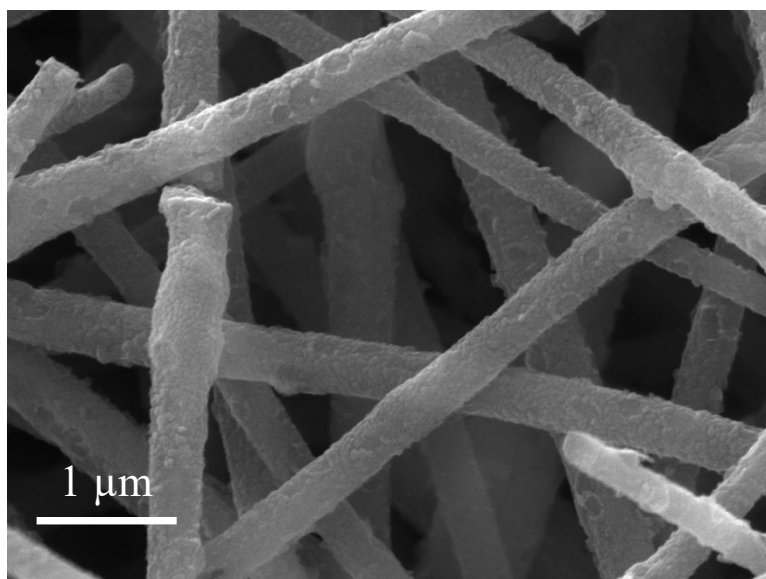


Figure S14. FESEM image of NVPCNF anode after 15000 cycles.

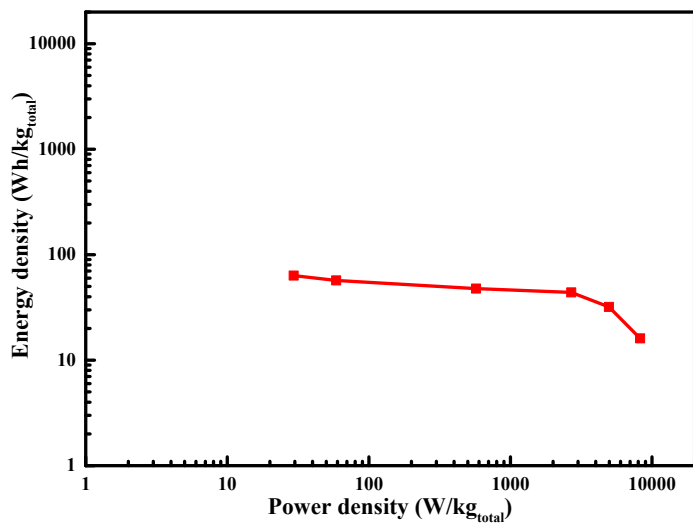


Figure S15. Ragone plot of the NVPCNF symmetric full cell.

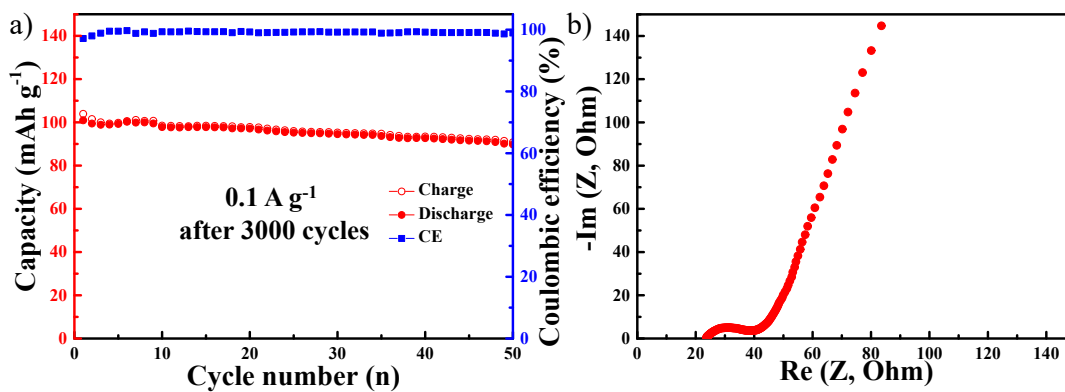


Figure S16. a) Cycling performance of NVP symmetric full cell at a current rate of 0.1 A g^{-1} after long-term cycling performance after 3000 cycles, b) Nyquist plot of the NVP symmetric flexible cell after cycling.

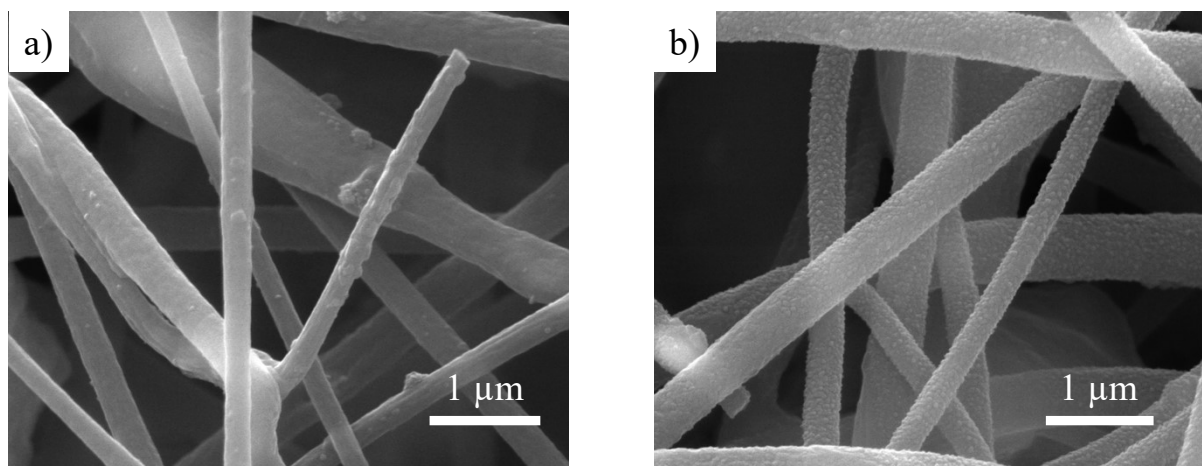


Figure S17. Exsitu FESEM image of a) cathode and b) anode of NVPCNF symmetric cell after 3000 cycles.